International Research Journal of Engineering and Technology (IRJET) e-ISSN: 2395-0056
Volume: 08 Issue: 03 | Mar 2021 www.irjet.net p-ISSN: 2395-0072

Selection of Turbulence Model for Analysis of Airfoil Wing using CFD

Shubham Goyal[1], Arnav Kulshreshtha[2], Shashank Singh[3]

[1]*Automobile Design Engineer, Aftersales Department, Bentley Motors Ltd, Crewe, England, United Kingdom*
[2]*Application Development Associate, Accenture Solutions Pvt Ltd, Pune, India*
[3]*Senior Engineer, Plant Integrity Department, L & T Chiyoda Ltd, Vadodara, India*

Abstract - *Analysis on an airfoil is the most trending topic in the field of aeronautics and it is a more versatile topic to dive in as the matter of fact that as you start varying the input conditions the interaction between the fluid and the airfoil body starts showing the drastic changes in its lift and overall efficiency. There is a wide range of research work on an airfoil using one or two turbulence models which do not depict the appropriate selection of model from the application point of view. This study mainly focuses on the selection of a suitable turbulence model based on the input available at the leading age of an airfoil profile. In this paper, it is analyzed how different airfoil shapes act in the varying condition of input parameters and how effective favorable results we can get using the most appropriate turbulence model. NACA2412, NACA2414, and NACA 2415 profiles are selected for this study and the coordinate data of all the profiles was picked from the official website of the National Advisory Committee for Aeronautics. Computational Fluid Dynamics and tool ANSYS Fluent 15.0 are used to conduct this study. Four different turbulence models standard k-ε, standard k-ω, Reynolds stress model & Transition k-kl-ω models are used to find the flow behavior and to compare the results with each other. This study is done for a wide range of angles of attack considering air as a fluid. For obtaining the results basic continuity equation, momentum equations, and all four different turbulence models are numerically calculated.*

Key Words: Turbulence models, Airfoil, Lift, Drag, Angle of Attack

1. INTRODUCTION

An airfoil is a different type of cross-sectioned body that has very smooth curved surfaces on the top and the bottom side. Airfoil is designed in such a way that it generates the desired lift and drag and this shape is the most popular in the application where any moving body interacts directly with the fluid stream. National Advisory Committee for Aeronautics has developed many airfoil sections to achieve the best efficiency, out of which three profiles are picked for the detailed study concerning the turbulence model. Due to the movement of an aircraft the lift and drag forces are generated. Lift force is the opposing force of the weight vector, which needs to act upward because of the downward direction of weight due to gravity. So, opposing lift force is generated by the airflow which creates the pressure difference between the top and bottom side of the wing. When wings face the airflow towards the direction of movement again one force generates at the surface of wings which is called drag force. Air resistance is the main cause of drag force which acts opposite to the movement of the aircraft. To balance the drag force propellers are used below the wings which creates an equal amount of thrust. During takeoff, thrust must overcome drag and lift must overcome the weight before the airplane can become airborne.

From the study of P. P. Sarkar et al. [1] the interaction between the fluid and structures is a very complex and costly method and it is the most challenging advanced engineering problem as well. These problems can be correctly tested in wind tunnels and through the live test but those tests are very dangerous as they include the life of a pilot or test rig operator. There are also some uncertain factors like geometry, flow properties, flow measurement complexity thus result from different laboratories differs as they use same experimental conditions and models, so after many decades of the wind tunnel testing Computational Fluid Dynamics (CFD) technique is developed with human involvement in early stages is reduced and the other one is to reduces the cost of operating real-time test. It is a bit complex but can produce equivalent results like wind tunnel testing. Nowadays CFD is the most popular way to solve any typical fluid engineering problem, thus Fluent has emerged as a widely used tool to simulate the flow analysis. J. Leary [2] performed CFD analysis on the blades of a wind turbine intending to analyze the lift and drag produced. The study concluded that the lift keeps on increasing with the angle but starts decreasing after a certain angle while the drag keeps on increasing continuously. The results suggested that the airfoils with greater camber will give a better lift. Z. Jaworski et al. [3] has shown comparison with a good similarity between RNG k-ε and standard k-ε models experimentally except for the trailing edge region. For the standard k-ε model, the turbulent quantities were found to more equivalent to the experimental data rather than the RNG k-ε model.

The study of A. Kulshreshtha et al. [4] shows the comparison between the coefficient of lift and drag v/s angle of attack of fluid for NACA 2412, NACA 2414, and NACA 2415. This work mainly focuses on the efficiency of the different airfoil sections at different AOA considering the standard k-ε model only. In the paper of V. Chumbre et al. [5] NACA2412 is found to be the best airfoil which generates the minimum drag force among the airfoil profiles NACA0012, NACA2412, NACA6409, NACA4412, NACAE387, hence it can be stated

that it has better fuel efficiency. C. Sagat [6] performed the analysis for the angle of attack from 0° to 20° on a low-velocity range of 12 meter/second to 15 meter/second. The results of the study show that the upper surface and lower surface of airfoil experience the lower negative coefficient of pressure for a higher angle of attack and lower angle of attack respectively. The coefficient of lift and drag majorly depends upon the velocity distribution and pressure distribution. S. Sarkar et al. [7] has also experimented on NACA2412. According to this work lift and drag, forces increase with increment in the range of angle of attack. At 5° angle analysis with the shear stress transport model, the results are most favorable and airfoil generates the maximum ratio of lift & drag forces. CFD analysis is conducted by A. Dash [8] on NACA0012 using a realizable k-ε turbulence model for AOA from 4° to 10°. The main observation of the study that the higher the angle of attack higher will be the lift force and its coefficient and on the other hand increment in drag force and its coefficient is quite low which is good.

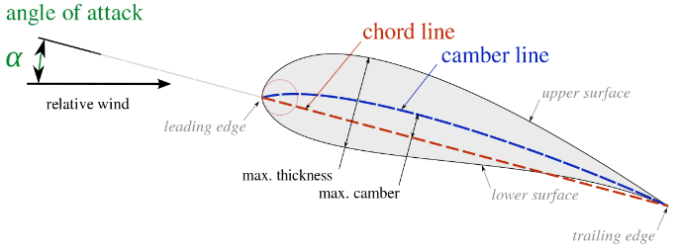

Fig -1: Airfoil Nomenclature

The most popular turbulence model in use is the k-ε model [9-12]. But apart from this model, there are other turbulence models available like k-ω turbulence model, Reynolds Stress turbulence model, Transition k-kl-ω turbulence model, etc. This study is based on all these models to compare and to find out which one is suited the best for the airfoil with minimum disturbance or fluctuations during the convergence. Modelling is a method by which we can predict the effect of turbulence. Turbulence modelling is always the most preferred solution of the actual fluid problems because in practicality there are very few significant examples of laminar flow.

1.1 Standard k-ε Turbulence Model

This is the two-equation model having k as kinetic energy and ε as turbulent dissipation. In the k-ε model, the viscosity is determined using a turbulent length scale. This model uses the gradient hypothesis to relate mean velocity and turbulent viscosity gradient. However, there is a lack of sensitivity to adverse pressure gradients. It is very easy to implement and valid for every type of turbulent flow. However, it is not good for complex shapes as it is a two-equation model.

1.2 Standard k-ω Turbulence Model

It is also a two-equation model in which the k is kinetic energy and ω is turbulent frequency. This will allow a user to get more accurate results near the wall with a low Reynolds number wall function based on grid spacing. It gives an outstanding performance, which is having a wall-bounded boundary layer at a low Reynolds number. Its separation is predicted early. Required great quality of the mesh.

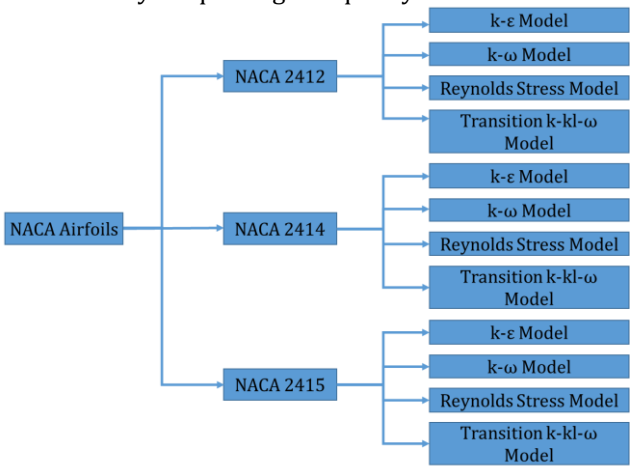

Fig -2: Methodology

1.3 Reynolds Stress Model

In fluid dynamics, the component of total shear tensor that is Reynolds stress is obtained from averaging operation over Navier-Stokes equations to account for turbulent fluctuations. For becoming any fluid to be turbulent, the flow velocity should be high enough but if the flow takes place in the circular pipe or any irregular surface or if there is more surface friction or sudden change in sections then eddies will be formed known as turbulent flow. Therefore, by altering the shape of any section, the effect can be minimized and Reynolds stress is the only specific factor in specific conditions.

1.4 Transition k-kl-ω Model

Walters and Leylek developed it. This is based on the Boussinesq hypothesis, which determines the Reynolds stress tensor. It perfectly works on the boundary layer phenomenon. It is a three-equation turbulence model.

2. GOVERNING EQUATIONS

2.1 Continuity Equation

$$\frac{\partial \rho}{\partial t} + \frac{\partial(\rho u)}{\partial x} + \frac{\partial(\rho v)}{\partial y} = 0 \qquad (1)$$

2.2 Momentum Equation

$$\frac{Du}{Dt} = X - \frac{1}{\rho}\frac{\partial \rho}{\partial x} + \frac{\mu}{\rho}\left[\frac{\partial^2 u}{\partial x^2} + \frac{\partial^2 u}{\partial y^2} + \frac{\partial^2 u}{\partial z^2}\right] \qquad (2)$$

$$\frac{Dv}{Dt} = Y - \frac{1}{\rho}\frac{\partial \rho}{\partial y} + \frac{\mu}{\rho}\left[\frac{\partial^2 v}{\partial x^2} + \frac{\partial^2 v}{\partial y^2} + \frac{\partial^2 v}{\partial z^2}\right] \qquad (3)$$

2.3 k-ε Equation

$$\frac{\partial \rho k}{\partial t} + div(\rho uk) = div\left[\left(\mu_t + \frac{\rho \mu_t}{\sigma_k}\right) gradk\right] + \rho \mu_t G - \rho \varepsilon \quad (4)$$

$$\frac{\partial \rho \varepsilon}{\partial t} + div(\rho u\varepsilon) = div\left[\left(\mu_t + \frac{\rho \mu_t}{\sigma_\varepsilon}\right) grad\varepsilon\right] + C_{1\varepsilon}\rho \mu_t \left(\frac{\varepsilon}{k}\right) - C_{2\varepsilon}\rho \frac{\varepsilon^2}{k} \quad (5)$$

2.4 k-ω Equation

$$\frac{\partial(\rho k)}{\partial t} + \frac{\partial(\rho \mu_j k)}{\partial x_j} = P - \beta^* \rho \omega k + \frac{\partial}{\partial x_j}\left[(\mu + \sigma_k \mu_t)\frac{\partial k}{\partial x_j}\right] \quad (6)$$

$$\frac{\partial(\rho \omega)}{\partial t} + \frac{\partial(\rho \mu_j \omega)}{\partial x_j} = \frac{\gamma}{v_t} P - \beta \rho \omega^2 + \frac{\partial}{\partial x_j}\left[(\mu + \sigma_\omega \mu_t)\frac{\partial \omega}{\partial x_j}\right] + 2(1 - F_1)\frac{\rho \sigma_{\omega 2}}{\omega}\frac{\partial k}{\partial x_j}\frac{\partial \omega}{\partial x_j} \quad (7)$$

2.5 Reynolds Stress Equation

$$\rho\left[\left(\frac{\partial \overline{u_i}}{\partial t} + \overline{u_j}\frac{\partial \overline{u_i}}{\partial x_j}\right)\right] = -\frac{\partial \bar{p}}{\partial x_i} + \frac{\partial}{\partial x_j}\left(\mu \frac{\partial \overline{u_i}}{\partial x_j} - \overline{\rho u_i' u_j'}\right) \quad (8)$$

2.6 Transition k-kl-ω Equation

$$\frac{Dk_T}{D} = P_{K_T} + R + R_{NAT} - \omega k_T - D_T \frac{\partial}{\partial x_j}\left[\left(v + \frac{\alpha_T}{\alpha_k}\right)\frac{\partial k_T}{\partial x_j}\right] \quad (9)$$

$$\frac{Dk_L}{D_t} = P_{K_L} - R - R_{NAT} - D_L + \frac{\partial}{\partial x_j}\left[v \frac{\partial k_L}{\partial x_j}\right] \quad (10)$$

$$\frac{D\omega}{D_t} = C_{\omega 1}\frac{\omega}{k_T}P_{K_T} + \left(\frac{C_{\omega R}}{f_w} - 1\right)\frac{\omega}{k_T}(R + R_{NAT}) - C\omega_2 \omega^2 + C\omega_3 f_\omega \alpha_T f_W^2 \frac{\sqrt{k_T}}{d^3} + \frac{\partial}{\partial x_j}\left[\left(v + \frac{\alpha_\gamma}{\alpha_\omega}\right)\frac{\partial \omega}{\partial x_j}\right] \quad (11)$$

3. COMPUTATIONAL IMPLEMENTATION

This study is completely performed using CFD. CFD simulations are generally performed in three steps named pre-processing, solution scheme, and post-processing. Solution setup and grid discretization play a very important role to get feasible simulation results. Computational domain creation and mesh generation comes under pre-processing. Boundary conditions are always the most important part because it defines the problem and creates virtually correct surroundings to run the simulations to capture the practically correct physics of the flow. Results of the study in form of different plots and contours are discussed in post-processing.

3.1 Geometry and Meshing

This is the first step of the CFD simulation process that helps in providing the best possible way to describe geometry. The computational domain is created on ANSYS Design Modeller. Cartesian coordinate points of different NACA profiles are imported to generate the boundaries. The analysis is done in 2D so there is no concept of creating the surfaces to cover the airfoil from a large surrounding. Just a big boundary box is created to define the environmental conditions of fluid.

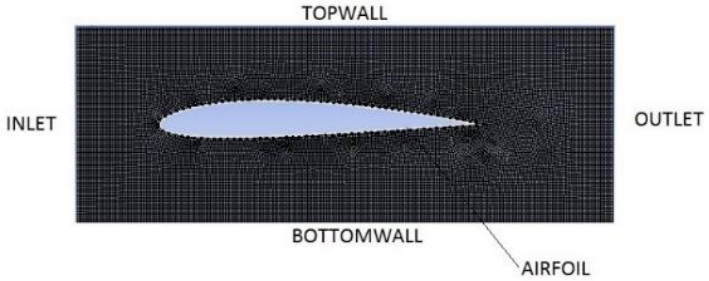

Fig -3: Discretized Computational Domain In The Vicinity Of Airfoil

Now the domain is discretized using a fine relevance centre. Medium smoothing was provided near the walls and a mesh with refined quality is created which is good enough dense to capture the flow in the close vicinity. Element size of 2.5631 e-004 meter and 2.5631 e-002 meter is provided for minimum and maximum face sizes respectively. The minimum edge length is kept 2.6 e-003m. Smooth inflation was used with a transition ratio of 0.272. A zoomed view of mesh elements in the vicinity of the airfoil is shown in fig. 3. The computational domain is discretized in a total of 23058 cells, 46660 faces, and 23602 nodes.

3.2 Solution Setup

As it is understood there is no way of compressible flow while analyzing an airfoil that is why a pressure-based steady-state study is done while simulating this problem. Different viscous models like k-epsilon, k-omega, Transition k-kl-omega, and Reynolds stress models are selected to cover all the cases of this study. This analysis is done by keeping the fluid air. The most important part of the solver settings is always boundary conditions which are shown in table 1.

SIMPLE pressure-velocity coupling is used with second-order spatial discretization of pressure, momentum, turbulence kinetic energy, and turbulence dissipation rate. The drag and lift coefficient monitors with residuals of 1.0 e-005 are set up for plotting on the console to get the maximum convergence. While initializing the solution we

should ensure the provided inlet conditions. Standard initialization is done followed by a run calculation command.

Table -1: Input Boundary Conditions

Model	• Standard k-ε equation • Standard k-ω equation • Reynolds Stress equation • Transition k-kl-ω equation
Inlet	Velocity – Inlet
Velocity Of Flow	30 meter/second
Density of Fluid	1.2 kilogram/meter^3
Fluid	Air
Outlet	Pressure – Outlet

4. RESULTS AND DISCUSSION

Since the study is conducted numerically and simulated using CFD completely on ANSYS so a wide range of angles of attack i.e. −5° to 20° is covered for all three profiles. While analyzing the data set generated by each simulation of all profiles corresponding to each turbulence model it is found that up to a certain range of angle of attack (AOA), all four models have shown a slight variation in between the lift and drag force readings. Thus to understand the behavior of turbulence, lift and drag forces are plotted combining the numerical values of all four models. In addition to this airfoil efficiency plots are also studied to get clarification on model selection.

Before explanation of the outcome of this work, one more important aspect related to this work is very much needed to be discussed and that is grid independent study. To check the dependency of the grid size on the quality of results and computational time is called grid independence study. This is required to select the correct size of mesh for simulation. The table below shows some figures about this study for NACA 2412.

Table -2: Grid Independency Test

Cases	No. of Elements	Airfoil Efficiency (Lift/Drag)			
		AOA 3°	AOA 4°	AOA 5°	AOA 6°
Case I	10878	24.28931	24.89934	17.94538	19.87954
Case II	16472	26.51037	27.01509	19.57274	21.89593
Case III	23058	27.03717	27.92067	20.05394	22.38363
Case IV	32659	27.03828	27.92118	20.05451	22.38395

From the table 2 it is found that with the increasing number of mesh elements from case I to case III there is a significant change in airfoil efficiency thus to increase the number of elements is fruitful. But from case III to case IV an increment in number of elements is 41.6% and correspondingly the increment in airfoil efficiency is just 0.001% to 0.004% which is not so great. In case IV output result is almost independent of higher mesh elements and computational time is increasing so much. So, from here onwards all the results are discussed considering case III mesh size.

At a glance all three graphical comparisons it is visible that k-epsilon and k-omega models have shown close results for the complete AOA range while Reynolds and Transition k-kl-omega models are deviating abruptly after 10° of the angle of attack. So, from here onwards a comparative study will be discussed keeping the k-epsilon model as a reference.

4.1 NACA 2412

Fig. 4, fig. 5 and fig. 6 show lift, drag, and airfoil efficiency (lift /drag) comparison plotted against the angle of attack. The graphical comparison shows two different behaviour before and after 10°.

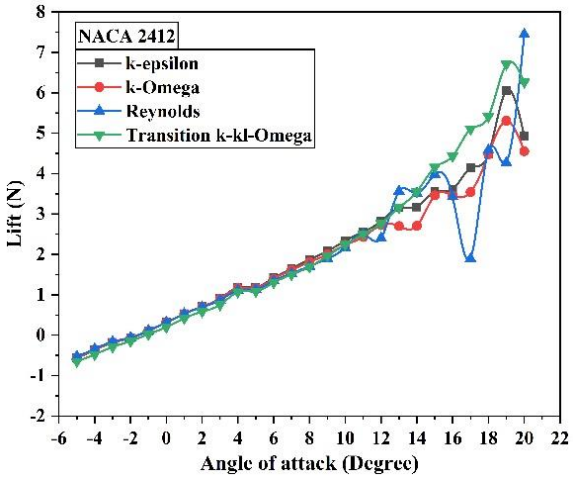

Fig -4: Graphical Comparison of Lift v/s AOA for NACA 2412

The value of lift and drag force is found almost similar in the initial range of AOA from -5° to 10° for k-epsilon and k-omega models but for the same range, a little more deviation is noticed for Reynolds and Transition k-kl-omega models. Similarly for AOA from -5° to 10° k-ε and k-ω models show close results for airfoil efficiency except for Reynolds & Transition k-kl-ω model. As it is known that high lift force and low drag force are always desired for most of the applications to get the best results from an airfoil shape, thus airfoil efficiency is required to be in consideration for further discussion. The average deviation of 3.7%, 5.7%, and 51.7% in airfoil efficiency is found (AOA: -5° to 10°) for the k-ω, Reynolds and Transition k-kl-ω models respectively.

A weird change is observed in the Transition k-kl-ω model throughout the angle range that's why results obtained from this cannot be reliable. For the range of AOA from 10° to 20° deviation of 16.8% and 20.6% is found for the k-ω & Reynolds model respectively. After 11° the values of lift and drag are fluctuating abruptly for Reynolds &

Transition k-kl-ω model hence airfoil efficiency is affected so much.

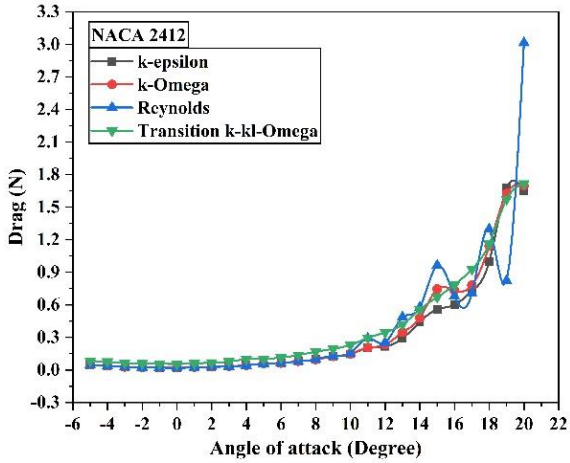

Fig -5: Graphical Comparison of Drag v/s AOA for NACA 2412

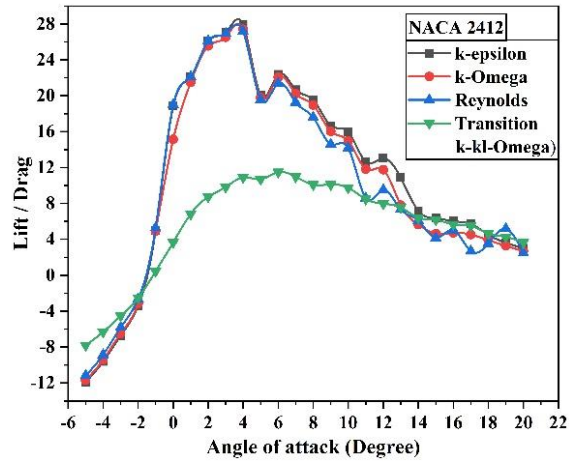

Fig -6: Graphical Comparison of Airfoil Efficiency (Lift/Drag) for NACA 2412

4.2 NACA 2414

The behavior of turbulence models is quite different in case of NACA 2414 but It has some similarity in regards to little and abrupt changes. Here k-ε and k-ω are in close resemblance to each other in case of lift, drag as well as airfoil efficiency. Reynolds model has shown drastic deviation in the lift and the drag forces both as compared to the Transition k-kl-ω model. Again comparative results are studied here considering the k-ε model as a reference.

Since airfoil efficiency matters that's why lift and drag numerical values are not discussed separately. The average deviation of 3.7%, 8 %, and 55 % in airfoil efficiency is found (AOA: -5° to 10°) for the k-ω, Reynolds and Transition k-kl-ω models respectively.

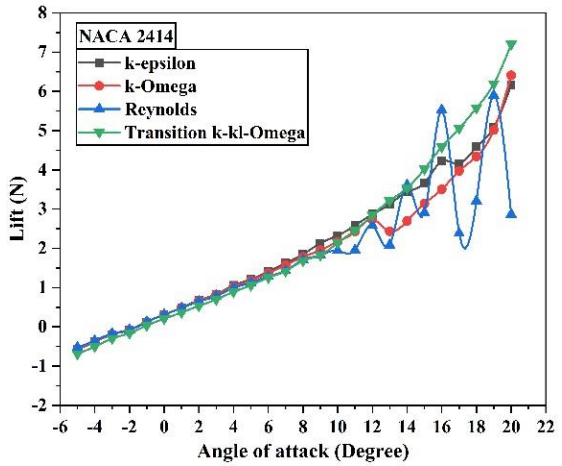

Fig -7: Graphical Comparison of Lift v/s AOA for NACA 2414

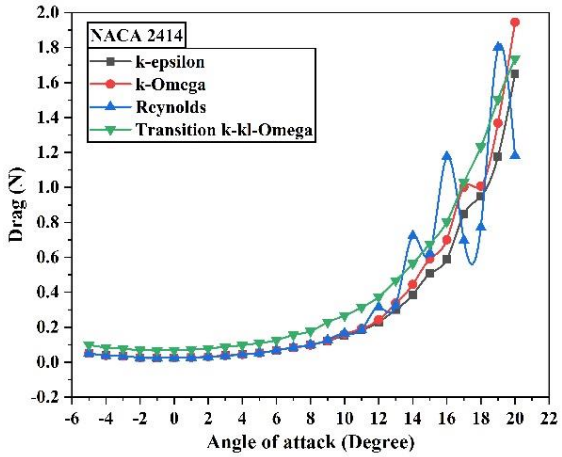

Fig -8: Graphical Comparison of Drag v/s AOA for NACA 2414

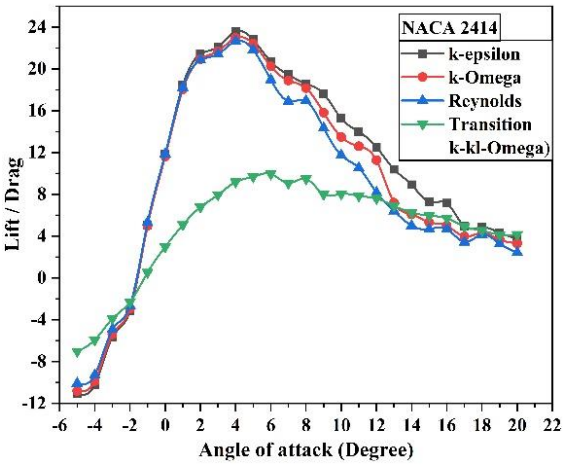

Fig -9: Graphical Comparison of Airfoil Efficiency (Lift/Drag) for NACA 2414

If drag force plot fig. 8 is closely monitored, it is found that for every angle of attack the value of drag produced by the Transition k-kl-ω model is at a much higher side than

that of other models, but at the same time for the AOA range of 10° to 20° highest lift force is also achieved. Because of greater drag force, the overall efficiency decreased drastically as compared to other models' results. The average deviation of 19.6%, 31.5%, and 18.4% in airfoil efficiency is found (AOA: 10° to 20°) for the k-ω, Reynolds and Transition k-kl-ω models respectively.

4.2 NACA 2415

It is observed that the behavior of turbulence models depends somewhere on the shape of the geometry and computational domain as well. The camber angle of airfoil NACA 2415 is greater than all the other cases here. More fluctuations in lift and draft are observed in this case. k-ε and k-ω models show very close results to each other again.

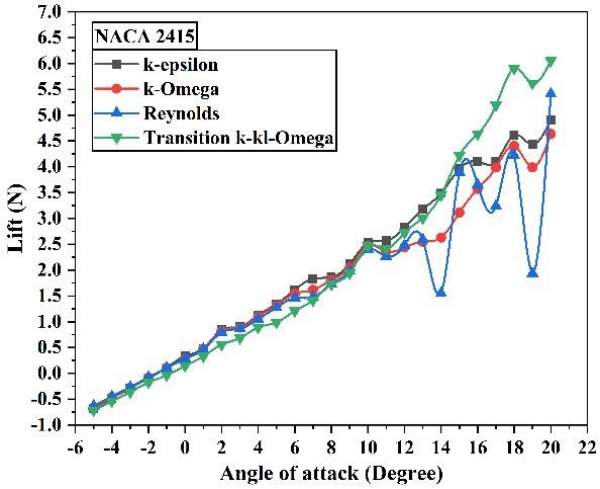

Fig -10: Graphical Comparison of Lift v/s AOA for NACA 2415

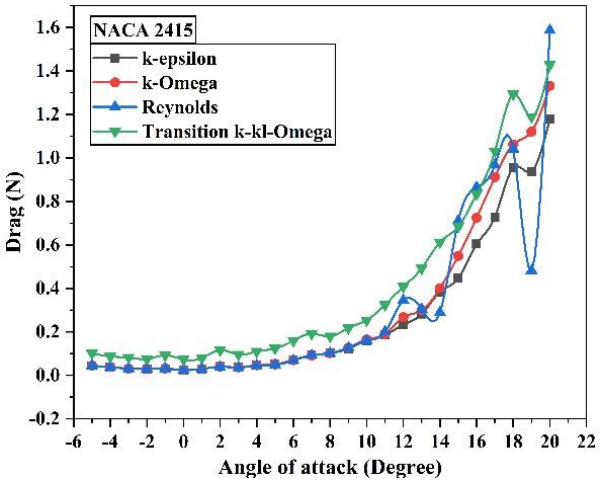

Fig -11: Graphical Comparison of Drag v/s AOA for NACA 2415

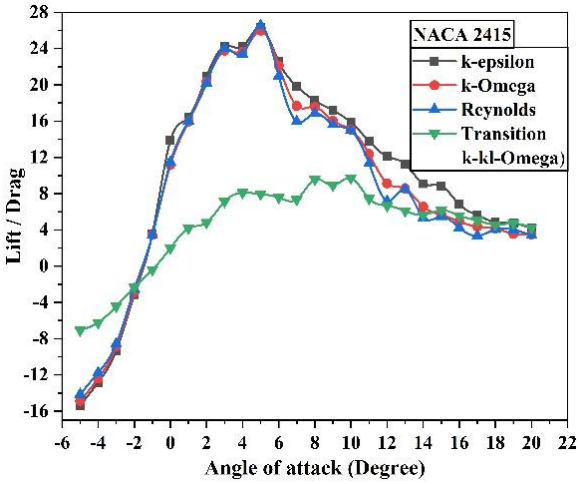

Fig -12: Graphical Comparison of Airfoil Efficiency (Lift/Drag) for NACA 2415

For the range of AOA from -5° to 10°, the deviation in airfoil efficiency is found 5.1%, 7.7%, and 62.7% for the k-ω, Reynolds and Transition k-kl-ω models respectively. Each time Transition k-kl-ω model has shown the highest lift although weird results of efficiency are noticed because of a very high amount of drag as compared to lift force. The average deviation of 22.8%, 29%, and 23.7% in airfoil efficiency is found (AOA: 10° to 20°) for the k-ω, Reynolds and Transition k-kl-ω models respectively.

5. CONCLUSIONS

As per numerical results obtained a detailed comparison is discussed for each NACA profile. Based on airfoil efficiency plots it can be decided which model should be chosen to conduct the simulation. Not only the best model selection but also the best range of angle of attack can also be decided with the help of efficiency graphs. It is clear from all the graphs of lift/drag ratio that airfoil efficiency is found at its best in the AOA range of 2° to 5°.

The transition k-kl-ω model has given the highest amount of lift in all cases but at the same time for the range of AOA from 2° to 5° a heavier drag force is observed and airfoil efficiency goes down. For the same range of angles from 2° to 5° all other models have sown the highest airfoil efficiency. If the k-epsilon model is monitored closely it is found that overall good efficiency is given by this model for a larger range of angle of attack. Even after 5° of angle k-epsilon model has produced a significantly lesser amount of drag as compared to lift force. In the range of AOA from 5° to 20° the k-epsilon model consistently provides the better efficiency as compared to k-omega and Reynolds models for all NACA profiles.

NOMENCLATURE

ρ – Density of fluid flowing (kg/m^3)

u – Density of fluid flowing (kg/m^3)

v – Density of fluid flowing (kg/m^3)

x – Component in *x*-direction

y – Component in *y*-direction

z – Component in *z*-direction

X – Body force in the x-direction (N)

Y – Body force in the y-direction (N)

μ_t – Eddy viscosity

k – Turbulent kinetic energy

ε –Turbulent dissipation rate

ω – Angular Velocity Vector

G – Turbulent generation rate

μ – Lame Constant (N/m^2)

μ_t - Eddy Viscosity

u_i – Displacement vector in x-direction (m)

u_i – Displacement vector in x-direction (m)

P – Precondition Matrix

γ – Interpolation Factor

v_t – Tangential component of velocity

σ_κ – Constant

σ_ε – Constant

$C_{1\varepsilon}$ – Constant

$C_{2\varepsilon}$ – Constant

ACKNOWLEDGEMENT

We would like to thank and express profound regards to Mr. Kuldeep Dagar, the senior researcher University of Nottingham, UK. Mr. Dagar spent countless hours directing us towards the successful completion of this work. Assistant professor Sanjeev Kumar Gupta, Mechanical Engineering department, GLA University, Mathura is also greatly acknowledged for arranging the CFD lab facility to complete this work.

REFERENCES

[1] P. P. Sarkar, L. Caracoglia, F. L. Haan Jr, H. Sato, J. Murakoshi, "Comparative and Sensitivity Study of Flutter Derivatives of Selected Bridge Deck Sections, Part 1: Analysis of Inter-Laboratory Experimental Data", Engineering Structures, vol. 31, pp. 158-169, 2009.

[2] J. Leary, "Computational Fluid Dynamics Analysis of a Low-Cost Wind Turbine", EPSRC, 2010.

[3] Z. Jaworski, K. N. Dyster, I.P.T. Moore, A. W. Nienow, M. L. Wyszynski, "The Use Of Angle-Resolved LDA Data To Compare Two Differential Turbulence Models Applied To Sliding Mesh Simulations In A Stirred Tank", Recents Progres en Genie des Procedes, vol. 11, pp. 187-194, 1997.

[4] A. Kulshreshtha, S. K. Gupta, P. Singhal, "FEM/CFD Analysis of Wings At Different Angle of Attack", Materials Today: Proceedings, vol. 26, part 2, pp. 1638-1643, 2020.

[5] V. Chumbre, T. Rushikesh, S. Umatar, S. M. Kerur, "CFD Analysis of Airfoil Sections", International Research Journal of Engineering and Technology (IRJET), vol. 5, issue 7, pp. 349-353, 2018.

[6] C. Sagat, P. Mane, B. S. Gawali, "Experimental and CFD Analysis of Airfoil at Low Reynolds Number", International Journal of Mechanical Engineering and Robotics Research, vol. 1, no. 3, pp. 277-283, 2012.

[7] S. Sarkar, S. B. Mughal, "CFD Analysis of Effect of Flow Over NACA 2412 Airfoil Through the Shear Stress Transport Turbulence Model", International Journal of Mechanical and Production Engineering, vol. 5, issue 7, pp. 58–62, 2017.

[8] A. Dash, "CFD Analysis of Wind Turbine Airfoil at Various Angles of Attack", IOSR Journal of Mechanical and Civil Engineering (IOSR-JMCE), vol. 13, issue 4, ver. II, pp. 18–24, 2016.

[9] A. L. Wensuslaus, A. J. McMillan, "Aerofoil Futter: Fluid-Mechanical Analysis and Wind Tunnel Testing", Journal of Physics: Conference Series 382, 2012.

[10] M. A. Fouad Kandil, A. O. Elnady, "Performance of GOE-387 Airfoil Using CFD", International Journal of Aerospace Sciences, 2017.

[11] A. Prabhakar, A. Ohri, "CFD Analysis on MAV NACA 2412 Wing in High Lift Take-Off Configuration for Enhanced Lift Generation", Journal of Aeronautics & Aerospace Engineering, vol. 2, issue 5, pp. 1-8, 2013.

[12] https://www.cfd-online.com/Forums/main/75554-use-k-epsilon-k-omega-models.html